JOURNAL OF MATERIALS SCIENCE 33 (1998) 5731–5737

Correlation of fiber pull-out strength and interfacial vibration damping techniques by micromechanical analysis

W. GU, S. L. KAMPE, G.-Q. LU
Department of Materials Science and Engineering, Virginia Polytechnic Institute and State University, Blacksburg, VA 24061, USA

H. F. WU
Advanced Technology Program, National Institute of Standards and Technology, Administration Building, Room A225, Gaithersburg, MD 20899, USA

Adhesion between fiber and matrix in fiber-reinforced polymer composites plays an important role both in controlling mechanical properties and in the overall performance of composites. This suggests that analytical and experimental methods to characterize the interface can be used to predict the mechanical performance of the material. To this end, vibration damping techniques have been used as a non-destructive method to evaluate interfacial effects on composites. According to the theory of energy dissipation, the quality of the interfacial adhesion can be evaluated upon separating the predicted internal energy dissipation associated with perfect adhesion from the measured internal energy dissipation of a composite system; this enables the quantification of interfacial adhesion. A micromechanics-based model for evaluating the adhesion between fiber and matrix from the damping characteristic of a cantilever beam was developed that shows an inverse relationship between the damping contributed by the interface and its adhesion strength. A simple optical system was used to measure the damping factor of unidirectional fiber-reinforced-polymer composites. Cantilever beam specimens containing either a single glass fiber or three types of single metallic wires embedded in an epoxy resin matrix were tested. A correlation was found between the measured interfacial adhesion strength directly from microbond pull-out tests and the micromechanics-based calculations from vibration damping experiments.

1. Introduction

It is well known that fiber-matrix interfacial adhesion strongly influences mechanical properties of a composite. The mechanical performance of the composite actually relies on effective load transfer from the matrix to the fiber through shear at the interfaces. Thus, a procedure capable of independently quantifying the interfacial adhesion could serve as an efficient and non-destructive means to evaluate the mechanical behavior of composite materials.

A large number of experimental techniques have been developed [1–15] for measuring interfacial adhesion in fiber-reinforced composites. Among these techniques, vibration damping potentially offers a sensitive and non-destructive way to evaluate details of the interfacial region in composites.

It is widely recognized that interfacial bonding or adhesion of a composite contributes to a change in energy-absorbing capacity, i.e., damping of the material. Thus, in analyzing the damping of a composite, it is important to consider not only the individual contributions from the component materials but also the energy dissipation attributable to the interfaces. Zorowski and Murayama [14] developed a method for measuring the quality of the interfacial adhesion in reinforced rubber through energy dissipation measurements, and they advanced the following simple relationships:

$$\tan\delta_{in} = \tan\delta_{comp} - \tan\delta_s \tag{1a}$$

$$\tan\delta_s = \frac{\tan\delta_f E_f V_f + \tan\delta_m E_m V_m}{E_m V_m + E_f V_f} \tag{1b}$$

where $\tan\delta_{in}$ is the damping factor attributable to the interface, $\tan\delta_s$ is the volume-compensated damping factor for the individual components of the composite ignoring any effects due to interfacial adhesion, and $\tan\delta_{comp}$ is the measured damping factor of the composite. E is the Young's modulus, and V represents volume fraction (subscripts f and m refer to the fiber and matrix, respectively). By measuring total system energy dissipation in terms of $\tan\delta_s$ and by using known or measured values of $\tan\delta$ and the dynamic moduli for each of the components, the dissipation due to interfacial adhesion can be determined; this in turn

should be related to the interfacial adhesion strength, τ. While theoretical and experimental analyses are reported that support the validity of a correlation between interfacial damping and interfacial adhesion strength [14–17], there is presently no direct relationship that quantitatively relates these two composite variables.

The properties obtained from unidirectional fiber-reinforced polymers (FRP) can be easily analyzed and modeled without considering other geometric parameters such as fiber length and fiber orientation. The study starts to develop a micromechanics model based on cantilever beam vibration to evaluate the adhesion strength between fiber and matrix from vibration damping data. Efforts are especially made to find a quantitative relationship between dynamic (vibration damping) and static (interfacial adhesion strength) adhesion measurements. The validity of the model will then be examined from experimental data obtained from a variety of single-fiber (-wire) unidirectional FRPs.

2. Model development

A schematic diagram of the model used to analyze theoretically the interfacial dissipative mechanism is depicted in Fig. 1. A single fiber of constant cross-section and properties is embedded in a matrix of lower modulus and of length equal to that of the fiber. Note that in Fig. 1 only loads parallel to the fiber axis are considered.

Based on the theory presented by Outwater [18], the analysis initially requires a calculation of stress distribution in the fiber when it is axially loaded. In several FRPs, the interfacial adhesion is primarily mechanical in nature and is often a consequence of the radial pressure, p, surrounding and acting on the fiber. Note that p is usually positive for polymer matrices/glass-fibers if it is a consequence of elevated temperature processing. Any relative movement between matrix and fiber is governed by the force required to overcome the frictional force in the longitudinal direction due to the radial pressure. A free-body diagram is shown in Fig. 2. By balancing the forces acting on the segment, the following general equation can be obtained:

$$\frac{dF_f}{dx}\,dx = \mu p \cdot 2\pi r_f\,dx \tag{2a}$$

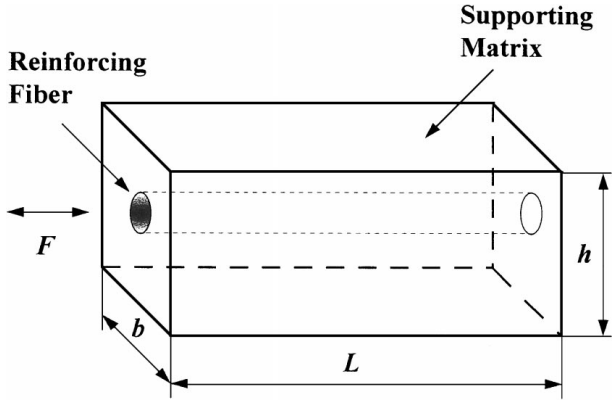

Figure 1 Simulated fiber reinforced composite model.

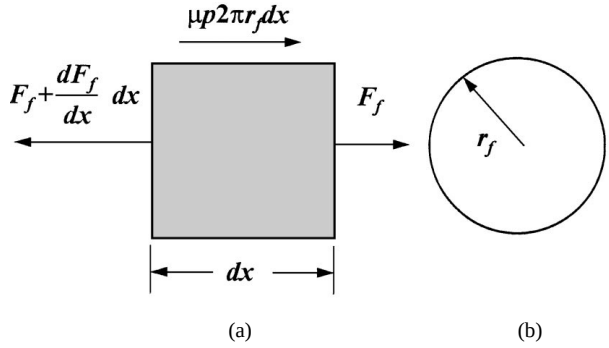

Figure 2 Forces acting on an element of a fiber: (a) force balance in a fiber element; (b) cross-section of the fiber.

where F_f is the axial force acting at the fiber, r_f is the fiber radius, and μ is the friction coefficient between fiber and matrix.

Similarly, if the interfacial debonding is caused by the force F_f during the stretching of the composite, then μp in Equation 2a can be replaced by the interfacial shear strength of the composite, τ, which is that necessary to pull the fiber from the matrix. The equation then becomes

$$\frac{dF_f}{dx}\,dx = \tau \cdot 2\pi r_f\,dx \tag{2b}$$

Equations 2a and b represent Coulomb friction and interfacial debonding caused by F_f, respectively. Note that in both cases, F_f is assumed to be constant, which is reasonable for small friction or a small debonding length. The total effect is obtained by superposition of the two equations. However, when both mechanisms are involved in the interfacial damping, the latter mechanism (interfacial debonding) will dominate because more energy dissipation is expected. Thus, the contributions due to the small elastic displacements described by Equation 2a can be neglected when slippage effects (2b) are active. Rearranging Equation 2b yields:

$$\frac{dF_f}{dx} = 2\pi r_f \tau \tag{3}$$

This equation can be easily solved to give

$$F_f = 2\pi r_f \tau x \tag{4}$$

The debonding length can thus be estimated from Equation 4:

$$x = \frac{F_f}{2\pi r_f \tau} \tag{5a}$$

For a cantilever beam, if there is an interfacial debonding, it likely occurs at the free end of the beam because shear strain (and shear stress) is high at that location [19]. In this case, the force balance is shown in Fig. 3.

The maximum debonding region is caused by the maximum load on fiber $F_f^{\max}$. When an alternating

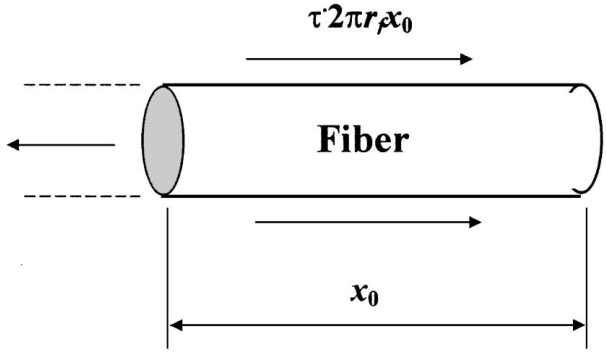

Figure 3 Free-body diagram of the free end of a cantilever beam.

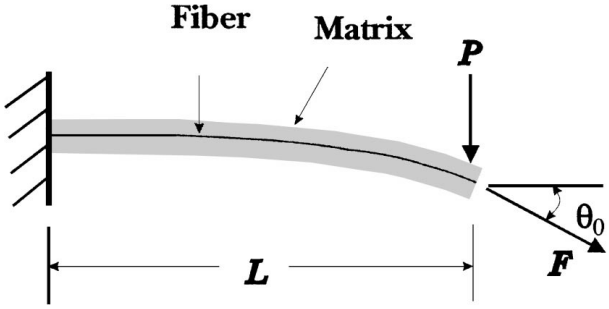

Figure 4 Force acting on a cantilever beam.

load is applied to the composite, such as in the case of vibration,

$$x_0 = \frac{F_f^{\max}}{2\pi r_f \tau} \tag{5b}$$

Forces F_f and $F_f^{\max}$ can be found from bending load P of a cantilever beam, as shown in Fig. 4. When the beam is deflected by an end-applied load P, the shear component of the load can be obtained as

$$F = F_f \approx P\theta_0 = \frac{P^2 L^2}{2E_c I_c} \tag{6}$$

where I_c is the moment of inertia of the composite beam. Therefore, the maximum load carried by fiber, $F_f^{\max}$, corresponding to the maximum bending load, $P_{\max}$, can be expressed quantitatively as

$$F_f^{\max} = \frac{P_{\max}^2 L^2}{2E_c I_c} \tag{7}$$

Provided the energy dissipation in a cycle ΔW is small compared to the maximum stored elastic energy W of the system, which is true for most vibration damping situations, the interfacial damping factor, $\tan\delta_{in}$, may be estimated by the following equation [20]

$$\tan\delta_{in} = \frac{\Delta W}{2\pi W} \tag{8}$$

Assuming the stress in the fiber gradually approaches the maximum value (or P gradually reaches to $P_{\max}$,) during a vibration cycle, interfacial debonding and slippage between fiber and matrix will dissipate energy. Because the integration is performed over a complete cycle about the origin, the energy dissipated per cycle is given by

$$\Delta W = 2F_f^{\max} x_0 \tag{9}$$

Substituting Equations 5b and 7 into Equation 9 yields

$$\Delta W = \frac{P_{\max}^4 L^4}{4\pi r_f \tau (E_c I_c)^2} \tag{10}$$

The potential energy W for a sample subjected to strain ε can be calculated as follows

$$W = \int_0^{\varepsilon_{\max}} (\sigma_c A_c)\cdot d\varepsilon L = \frac{1}{2} A_c L E_c \varepsilon_{\max}^2 \tag{11a}$$

where L is the sample length, and σ_c, A_c, and E_c are the stress, cross-sectional area, and Young's modulus of the composite, respectively. For a cantilever beam, $\varepsilon_{\max} = P_{\max}^2 L^4/15(E_c I_c)^2$ [21], and we obtain

$$W = \frac{1}{2} A_c L E_c \left(\frac{P_{\max}^2 L^4}{15(E_c I_c)^2}\right)^2 \tag{11b}$$

By substituting Equations 10 and 11b into Equation 8, and by knowing that $I_c = bh^3/12$, we obtain

$$\tan\delta_{in} = \frac{25E_c b h^5}{64\pi^2 \tau r_f L^5} \tag{12}$$

where b is the sample width and h is sample thickness.

If the number of fibers that can cause debonding in the composite is n, Equation 12 will be changed to

$$\tan\delta_{in} = n\frac{25E_c b h^5}{64\pi^2 \tau r_f L^5} \tag{13}$$

For the vibration of a cantilever beam, E_c can be calculated according from vibration theory [22]

$$E_c = \frac{m_c \omega_c^2 L^4}{1.875^4 I_c} = \frac{12(\rho_f V_f + \rho_m V_m)\omega_c^2 L^4}{1.875^4 h^2} \tag{14}$$

where ω_c is the resonant frequency at the first mode of vibration, m_c is the mass of the composite per unit length, and ρ is the density.

Substituting Equation 14 into Equation 13 we obtain, after rearranging,

$$\tau = B\frac{nbh^3(\rho_f V_f + \rho_m V_m)\omega_c^2}{\tan\delta_{in} r_f L} \tag{15}$$

where

$$B = \frac{75}{16 \times 1.875^4 \pi^2}$$

Equation 15 clearly shows the inverse relationship between $\tan\delta_{in}$ and τ, which is as expected.

3. Experimental verification

3.1. Composite sample preparation

Single-fiber composite specimens are commonly used to evaluate interfacial adhesion by methods such as the pull-out test. A single-fiber reinforced composite sample has been likewise used in the present study because vibration-derived interfacial adhesion strength can be directly compared to values obtained from the single-fiber stress analysis obtained from a fiber pull-out test. However, the diameters of fibers should be large enough such that the fiber volume fraction of the single-fiber reinforced composite is significant. The resolution of the vibration damping setup used in the experiment is then sufficient to detect the interfacial damping of a single-fiber reinforced composite. Beside glass fibers with a 0.12 mm diameter, copper, molybdenum, and tungsten wires were also used as reinforcements in epoxy matrices for single-fiber composite specimens. The exact diameters of the metallic wires were 0.1 mm for both copper and tungsten and 0.127 mm for molybdenum. Each metallic wire used had a unique Young's modulus (copper, molybdenum, and tungsten have Young's moduli about 100, 200, and 300 GPa, respectively), and likely, different adhesion strengths with the epoxy resin. As such, both vibration damping and microbond specimens were fabricated and used for measuring the interfacial damping and the interfacial adhesion strength.

Sample preparation was conducted according to the procedure suggested by the manufacturer of the epoxy resin. Epon 828^{TM} (a trademark of Shell Chemical Company) epoxy resin (100 parts by weight) was mixed with mPDA (1, 3-Phenylenediamine flakes) curing agent (14.5 parts by weight) when mPDA was completely melted at 70 °C. The mixture was placed into a warm vacuum oven (50 °C) for 30 min to remove gas bubbles introduced during the mixing. The mixture was then used for preparing the single-fiber (wire) composite microbond pull-out or vibration damping specimens. For the microbond pull-out specimens, an axisymmetric drop of epoxy was placed onto the fibers (wires) using a small-diameter steel needle. For the fabrication of the vibration damping beam specimens, epoxy was poured into a mold with a size of 30 mm × 3 mm × 1 mm, into which the single-fibers (wires) were placed. In both instances, the prepared specimens were cured for 2 h at 75 °C and 2 h at 125 °C. For all of the metallic wire-reinforced polymer composites used in the current study, the wires were not only supplied in as-received condition but also coated with silicone mold release to create a weak wire-matrix interface.

3.2. Optical setup

A schematic of the optical setup designed to measure the deflection and vibration dynamics of a cantilever beam is shown in Fig. 5. The apparatus consists of a 1 mW solid-state laser (670 nm), a mirror, a beam splitter, and a position sensitive photodetector. A sample is mounted by clamping it vertically between two plates such that the protruding part forms a cantilever beam. An electronically triggered pin is used to generate an initial deflection on the sample; vibration of the sample is initiated by retracting the pin. Vibration curves are obtained by reflecting a laser beam off the sample to the photodetector.

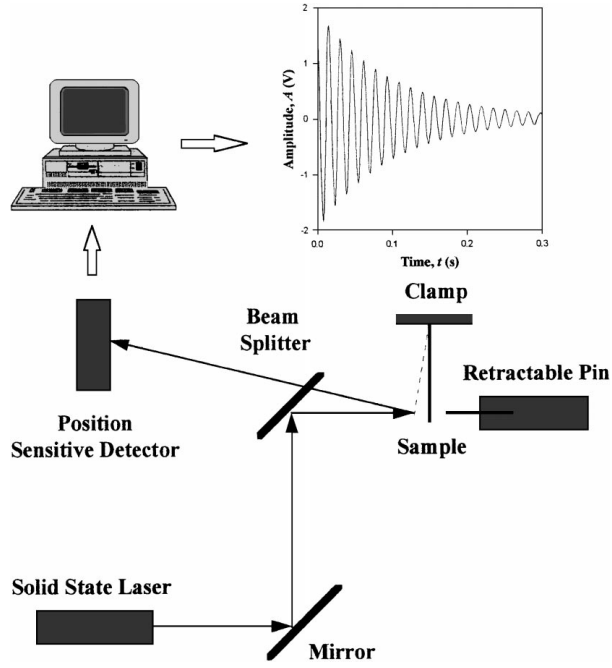

Figure 5 Schematic diagram of the optical system.

The damping factor, $\tan\delta$, is calculated from decaying-oscillatory damping curve using the relationship [22]

$$\tan\delta = \frac{\ln(A_0/A_m)}{m\pi} \tag{16}$$

where m is the number of cycles of the vibration, A_0 is the amplitude of the first vibration, and A_m is amplitude of the Mth vibration. The term $\ln(A_0/A_m)/m$, also known as the logarithmic decrement Δ, can be obtained by fitting the experimental data to the following formula [22]

$$A(t) = B_0 \exp(-\zeta\omega_r t)\cos(\omega_d t - \phi) + B_1 \tag{17}$$

where ω_r is the resonant frequency of vibration, $\zeta = \Delta/\sqrt{(2\pi)^2 + \Delta^2} \approx \Delta/2\pi$ when damping is small; $\omega_d = (1-\zeta^2)^{1/2}\omega_r$, B_0, B_1, and ϕ are constants.

4. Experimental results and discussion

The interfacial adhesion strength measurements obtained from the microbond single-fiber (-wire) pull-out tests are summarized in Table I. The measurements show clearly that all silicone mold release-coated wires exhibit lower interfacial adhesion strengths. The experimental values listed in Table I are the averages obtained from at least twenty microbond specimens.

Fig. 6 shows a typical example of the vibration damping curve of a single-glass-fiber-reinforced composite sample, which was obtained from the optical system described in section 3.2. The value of $\tan\delta$ was found to be 39.8×10^{-3}, which is typical for this material system at the fixed resonant frequency. Other experimental

TABLE I The interfacial adhesion strength obtained from the microbond pull-out tests

Fibers (Wires)	Fiber Diameter (μm)	Interfacial Adhesion Strength, $\tau_{measure}$ (KPa)
Mo	127	1071 (±315)*
Mo (coated with silicone mold release)	127	788 (±396)
Cu	100	1263 (±324)
Cu (coated with silicone mold release)	100	830 (±317)
W	100	1296 (±498)
W (coated with silicone mold release)	100	569 (±393)
Glass	120	329 (±207)

*Numbers in parenthesis represent ±1 standard deviation.

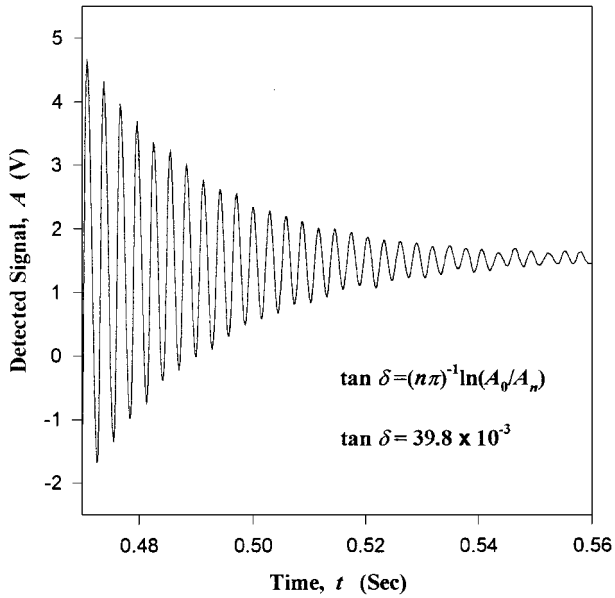

Figure 6 An example of the vibration damping curves obtained from single-glass-fiber reinforced composite samples using the optical system.

results are summarized in Table II, which are averages obtained from at least five specimens.

It is important to note from Tables I and II that the overall vibration damping characteristics and resonant frequencies of the tested specimens depend on sample dimensions. It can be seen that there is no obvious relationship between the overall damping factor of the composites and the interfacial adhesion strength. Therefore, it is necessary to separate the contribution of energy dissipation from the component materials and the interface to determine the correspondence of the interfacial damping and interfacial adhesion strength. It is known that Equation 15 can be used for this purpose. However, prior to applying Equation 15 to calculate the interfacial damping contribution, it is necessary to know the values of certain parameters, including the Young's modulus of the composites, and the Young's moduli and tan δ for each component. In the current study, some values were obtained by experiment, while some data were obtained from the literature.

From the Bernoulli–Euler beam equation [22], it can be shown that the Young's modulus, E, of the material is related to its frequency of vibration. The equation used for calculating E for a beam specimen is as follows [22]:

$$E = \frac{12\rho\omega_r^2 L^4}{1.875^4 h^2} \tag{18}$$

where ω_r is the resonant frequency of the first mode of vibration, L and h are the length and the thickness of the beam, and ρ is the beam density. The density of the epoxy resin is reported as 1.115 g/cm^3 [23] for the Epon 828 epoxy resin. Rule of mixtures (ROM) was used to obtain the beam density for all composite beams.

It has been reported that the damping factor also varies with frequency [24]. By changing the beam length, an identical natural frequency (or resonant frequency) was obtained for the single-component materials, which was comparable to the frequencies of the tested composites. The Young's moduli and damping factors measured from the optical vibration damping system are summarized in Table III. The average

TABLE III Densities, Young's moduli, and damping factors of component materials of single-fiber (wire) reinforced composites

	ρ (g/cm^3)	E (GPa)	tan δ (10^{-3})
Epon 828 epoxy resin	1.115[1]	3.0 (±0.2)[2]	43.1 (±1.8)
Copper	8.93[3]	98 (±7)	3.20(±0.26)
Molybdenum	10.22[3]	220 (±11)	3.20 (±0.12)
Tungsten	19.3[3]	315 (±16)	2.90 (±0.19)
Glass	2.54[4]	60[5]	1.0[4]

[1]Obtained from reference [62].
[2]Numbers in parenthesis represent ±1 standard deviation.
[3]Products of Alfa® Aesar®.
[4]Obtained from reference [48].
[5]Product Data provided by Owens Corning.

TABLE II Measured resonant frequencies and damping factors of single-fiber (wire) reinforced composites

Fibers	Width, b (mm)	Thickness, h (mm)	ω_r (s^{-1})	tan δ_c (10^{-3})
Mo	2.871 (±0.117)**	0.991 (±0.040)	2754 (±115)	43.1 (±2.78)
Mo*	2.898 (±0.106)	0.960 (±0.039)	2759 (±133)	40.6 (±3.78)
Cu	2.897 (±0.111)	0.908 (±0.046)	2897 (±137)	45.5 (±1.56)
Cu*	2.993 (±0.050)	0.923 (±0.036)	2902 (±169)	47.4 (±1.62)
W	2.912 (±0.060)	0.798 (±0.043)	2514 (±130)	41.9 (±2.15)
W*	2.851 (±0.068)	0.838 (±0.036)	2829 (±93)	37.7 (±4.29)
Glass	2.858 (±0.096)	0.857 (±0.075)	2427 (±195)	39.8 (±1.06)

*With silicone mold release.
**Numbers in parenthesis represent ±1 standard deviation.

TABLE IV Damping factors contributed from interface of single-fiber (wire) reinforced composites

Fibers	Width, b (mm)	Thickness, h (mm)	$\tan\delta_{in}$ (10^{-3})
Mo	2.871 (±0.117)**	0.991 (±0.040)	0.58 (±0.27)
Mo*	2.898 (±0.106)	0.960 (±0.039)	0.79 (±0.30)
Cu	2.897 (±0.111)	0.908 (±0.046)	0.58 (±0.18)
Cu*	2.993 (±0.050)	0.923 (±0.036)	1.29 (±0.51)
W	2.912 (±0.060)	0.798 (±0.043)	0.34 (±0.13)
W*	2.851 (±0.068)	0.838 (±0.036)	1.67 (±0.76)
Glass	2.858 (±0.096)	0.857 (±0.075)	0.80 (±0.21)

*With silicone mold release.
**Numbers in parenthesis represent ±1 standard deviation.

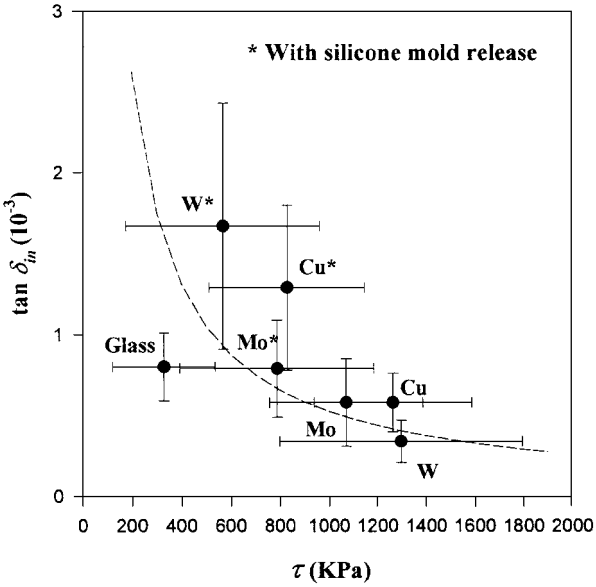

Figure 7 The relationship between $\tan\delta_{in}$ and interfacial adhesion strength for single-fiber (wire) reinforced composites.

values of the data listed in Table III were used to calculate $\tan\delta_{in}$ based on Equation 15. The results are given in Table IV.

When comparing values of $\tan\delta_{in}$ listed in Table IV with the measured interfacial adhesion strength τ_{measure} shown in Table I, it can be obviously seen that there exists an inverse relationship between the two parameters (refer to Fig. 7).

The crack was found at the free end of the cantilever, and it moved inward during the vibration, which is consistent to the assumption made in the model development [25].

After applying the derived model, the interfacial adhesion strength can be calculated from interfacial damping value $\tan\delta_{in}$ according to Equation 15. For the single-fiber (-wire) reinforced epoxy composites used in the current study, the number of debonded fibers n is simply equal to 1. By using the necessary data listed in Tables III and IV, predicted values of τ_{calc} were obtained, which are given in Table V. By comparing the values of τ_{calc} in Table V and τ_{measure} in Table I, it is found that the experimental results fairly agree with the prediction. The comparison of the results is also graphically illustrated in Figs 8 and 9.

It is interesting to note that different fibers (wires) have various adhesion properties with Epon 828$^{\text{TM}}$

TABLE V Damping factors contributed from interface and calculated interfacial adhesion strength of single-fiber (wire) reinforced composites

Fibers	Fiber Diameter (μm)	$\tan\delta_{in}$(10^{-3})	τ_{calc} (KPa)
Mo	127	0.58 (±0.27)**	1145 (±480)
Mo*	127	0.79 (±0.30)	793 (±458)
Cu	100	0.58 (±0.18)	1471 (±736)
Cu*	100	1.29 (±0.51)	706 (±231)
W	100	0.34 (±0.13)	1328 (±495)
W*	100	1.67 (±0.76)	482 (±224)
Glass	120	0.80 (±0.21)	419 (±161)

*With silicone mold release.
**Numbers in parenthesis represent ±1 standard deviation.

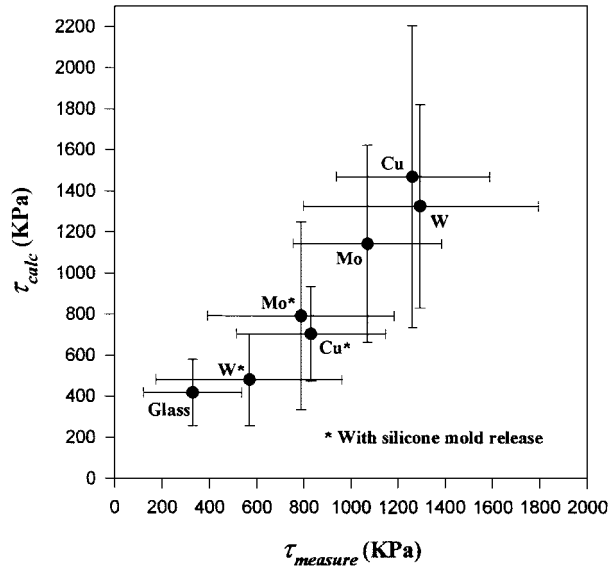

Figure 8 Comparison of average values of τ_{calc} and τ_{measure} of single-fiber (wire) reinforced composite. Error bars represent ±1 standard deviation.

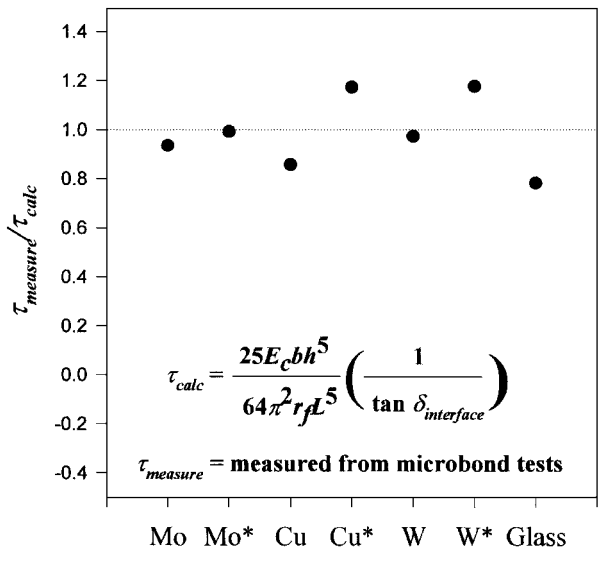

Figure 9 Comparison of average values of τ_{calc} and τ_{measure} of single-fiber (wire) reinforced composites with another method to analyze the data.

epoxy resin used in the current study. It is understandable that the wires coated with silicone mold release exhibit a lower interfacial adhesion strength because of the weakening of the wire-matrix interface. The reason for a stronger interfacial adhesion in metallic wire-reinforced composites than that in glass-fiber reinforced composite can be attributed to the different surface roughness of the fiber or wires. The glass fiber has a smoother surface than metallic wires, resulting in poorer interlocking between fiber and epoxy resin. This could be the main reason for lower interfacial adhesion strength.

5. Conclusions

Adhesion at the fiber-matrix interface in fiber-reinforced composites plays an important role in controlling the mechanical properties and overall performance of composites. Among the many available tests applicable to composite interfaces, the vibration damping technique has the advantage of being nondestructive as well as highly sensitive. A micromechanics model was developed to correlate interfacial damping factor $\tan \delta_{in}$ and interfacial adhesion strength τ for the damping of unidirectional fiber-reinforced composites in the shape of cantilever beams. An inverse relationship between $\tan \delta_{in}$ and τ was found.

A simple optical system was constructed for measuring the damping factor of unidirectional fiber-reinforced-polymer (FRP) composites in the shape of cantilever beams. Adhesion at fiber-matrix interfaces in single-fiber (-wire) reinforced epoxy-resin was characterized by using the system.

The single-fibers (-wires) used in the current study included glass, copper, molybdenum, and tungsten. The interfacial adhesion strengths measured from microbond pull-out tests are compared to measured interfacial damping factor of a single-fiber (-wire) composite cantilever beam. An inverse relationship between the damping characteristics of the fiber-matrix interface and interfacial adhesion strength of composites was found from the experimental results, which is consistent with the derived micromechanics model. It is noted that the interfacial adhesion strength is dependent on the roughness of the fiber surface. A smooth fiber surface in the composite may lead to a low interfacial adhesion strength.

References

1. L. T. BROUTMAN, *Polymer Eng. Sci*. **6** (1966) 1.
2. M. R. PIGGOTT in "*Interfacial Phenomena in Composite Materials*," edited by I. Verpoest and F. Jones (Butterworth-Heinemann, Oxford, 1991) p. 3.
3. A. KELLY and W. R. TYSON, *J. Mech. Phys. Solid* **13** (1965) 329.
4. B. MILLER, P. MURI and L. REBENFELD, *Comp. Sci. Tech*. **28** (1987) 17.
5. J. P. FAVRE and J. PERRIN, *J. Mat. Sci*. **7** (1972) 1113.
6. J. F. MANDELL, E. J. H. CHEN and F. J. MCGARRY, *Int. J. Adhesion Adhesives* **1** (1980) 40.
7. J. F. MANDELL, D. H. GRANDE, T. H. TSIANG and F. J. MCGARRY in "Composite Materials, Testing and Design, ASTM STP 893" (American Society for Testing and Materials, 1986) p. 87.
8. H. F. WU and M. K. FERBER, *J. Adhesion* **45** (1994) 89.
9. N. J. WADSWORTH and I. SPILLING, *Brit. J. Appl. Phys*. **1** (1968) 1049.
10. L. T. DRZAL, *SAMPE J*. **19** (1983) 7.
11. A. N. NETRAVALI, Z.-F. LI, W. SACHSE and H. F. WU, *J. Mat. Sci*. **26** (1991) 6631.
12. M. MIWA, T. OHSAWA and K. TAHARA, *J. Appl. Polymer Sci*. **24** (1980) 795.
13. U. GAUR and B. MILLER, *Comp. Sci. Technol*. **34** (1989) 35.
14. C. F. ZOROWSKI and T. MURAYAMA, "*Proceedings of the 1st International Conference on Mechanical Behavior of Materials*" **5** (Society of Materials Science, Kyoto, Japan, 1972) p. 28.
15. H. F. WU, W. GU, G.-Q. LU and S. L. KAMPE, *J. Mater. Sci*. **32** (1997) 1795.
16. T. MURAYAMA, "*Dynamic Mechanical Analysis of Polymeric Material*" (Elsevier, Amsterdam, 1978).
17. P. S. CHUA, *Polym. Comps*. **8** (1987) 308.
18. J. O. OUTWATER, Jr., *Modern Plastics* **March** (1956) 56.
19. M. MASUKO, Y. ITO and K. YOSHIDA, *Bulletin of the JSME* **99** (1973) 1421.
20. B. J. LAZAN, "Damping of Materials and Members in Structural Mechanics" (Pergamon Press, 1968).
21. J. P. DEN HARTOG, "Mechanical Vibrations" (McGraw-Hill, New York, 1985).
22. L. MEIROVITCH, "Elements of Vibration Analysis," edited by B. J. Clark and M. E. Margolies (McGraw-Hill, 1975).
23. M. WELLER and H. LEDBETTER, *J. Mater. Res*. **5** (1990) 913.
24. R. F. GIBSON and R. PLUNKETT, *J Compos. Mat*. **10** (1976) 325.
25. W. GU, Doctoral Thesis, Virginia Polytechnic Institute and State University (1997).

Received 18 June
and accepted 6 August 1998